

Lymphocyte subsets in Atlantic cod (*Gadus morhua*) interrogated by single-cell sequencing

Naomi Guslund (✉ naomi.croft@gmail.com)

University of Oslo <https://orcid.org/0000-0002-8010-0065>

Anders Krabberød

University of Oslo <https://orcid.org/0000-0001-9481-8396>

Simen Nørstebø

Norwegian University of Life Sciences

Monica Solbakken

Norwegian University of Life Sciences,

Kjetill Jakobsen

University of Oslo <https://orcid.org/0000-0002-8861-5397>

Finn-Eirik Johansen

University of Oslo

Shuo-Wang Qiao

University of Oslo

Article

Keywords: Atlantic Cod¹, single-cell sequencing², CD8-negative T lymphocytes³, monocyte chemotactic protein 14, scavenger receptor m1305

Posted Date: February 18th, 2022

DOI: <https://doi.org/10.21203/rs.3.rs-1342445/v1>

License:   This work is licensed under a Creative Commons Attribution 4.0 International License.

[Read Full License](#)

Version of Record: A version of this preprint was published at Communications Biology on July 11th, 2022. See the published version at <https://doi.org/10.1038/s42003-022-03645-w>.

Lymphocyte subsets in Atlantic cod (*Gadus morhua*) interrogated by single-cell sequencing

Authors and affiliations:

Naomi Croft Guslund^{1*}, Anders K. Krabberød^{1,2}, Simen F. Nørstebø³, Monica Hongrø Solbakken⁴, Kjetill S. Jakobsen⁴, Finn-Eirik Johansen⁵, Shuo-Wang Qiao^{6*}

¹Centre for Ecological and Evolutionary Synthesis, Department of Biosciences and the Department of Immunology, University of Oslo, Oslo, Norway

²Section for Genetics and Evolutionary Biology, Department of Biosciences and the Department of Immunology, University of Oslo, Oslo, Norway

³Department of Paraclinical Sciences, Faculty of Veterinary Medicine, Norwegian University of Life Sciences, Ås, Norway

⁵Section for Physiology and Cell Biology, Department of Biosciences, University of Oslo, Oslo, Norway

⁶Department of Immunology, Institute of Clinical Medicine, University of Oslo, Oslo, Norway

Correspondence

*Naomi Croft Guslund – n.c.guslund@ibv.uio.no

*Shuo-Wang Qiao - s.w.qiao@medisin.uio.no

Keywords: Atlantic Cod₁, single-cell sequencing₂, CD8-negative T lymphocytes₃, monocyte chemotactic protein 1₄, scavenger receptor *m130*₅

Abstract

Atlantic Cod (*Gadus morhua*) has lost the *major histocompatibility complex class II* presentation pathway. We recently identified CD8-positive T cells, B cells, and plasma cells in cod, but further characterization of lymphocyte subsets are needed to elucidate immune adaptations triggered by the absence of CD4-positive T lymphocytes. Here we use single-cell RNA sequencing to examine the lymphocyte heterogeneity in Atlantic cod spleen. We describe five TCR-positive T cell subsets and eight BCR-positive B cell subsets and propose a B cell trajectory of differentiation. Notably, we identify a significant subpopulation of T cells that are CD8-negative. Most of the CD8-negative T lymphocytes highly express the homolog of *monocyte chemotactic protein 1b*, and another subset of CD8-negative T lymphocytes express the homolog of the scavenger receptor *m130*. Uncovering the multiple lymphocyte cell sub-clusters reveals the different immune states present within the B and T cell populations, building a foundation for further work.

1 Introduction

Comparative studies of a limited number of model organisms have led to a commonly held view that the adaptive immune system common to jawed vertebrates has remained largely unchanged since its origin some 500 million years ago [1, 2]. More recent studies of non-model organisms have begun to challenge this view, as exemplified by the Atlantic cod (*Gadus morhua*). The Atlantic cod belongs to a growing number of identified teleost species that have lost substantial parts of the adaptive immune system. The Gadiformes order, of which the Atlantic cod is one of the most prevalent species, lost the entire set of *major histocompatibility complex (MHC) class II* genes around 80-100 million years ago [3, 4]. The *cd4* gene is also non-functional, and thus cod does not have CD4-positive T cells, which are known to play a pivotal role in raising a humoral immune response in mammalian immune systems. Despite its ‘unusual’ immune system, cod is a prolific species and in its natural environment is not more prone to diseases than other teleosts with more ‘conventional’ immune systems [5]. Although it has proven difficult to elicit specific antibody responses by immunisation,

51 Atlantic cod does display specific and long-term protective memory in vaccination studies [6-10]. Thus,
52 Atlantic cod has a well-functioning immune system in the absence of CD4-positive T cells, but the
53 mechanisms for generating specific immune memory, if it exists in cod, must differ from the well-
54 known model based on collaboration between B cells and CD4-positive T cells, although this model is
55 in general not validated in teleosts.

56 As a first step towards understanding the workings of the immune system of Atlantic cod, we
57 have used single-cell transcriptomics to characterise the immune cell composition. In a previously
58 published study, we analysed the transcriptomic profile of some seven thousand immune cells
59 sampled from the spleen and blood of two Atlantic cod [11]. We identified major immune-cell
60 populations (T cells, B cells, plasma cells, macrophages, and granulocytes) and non-immune cells
61 (erythrocytes, thrombocytes, and spleen stromal cells), as well as minor populations of cells such as
62 dendritic cells and GATA3⁺ cytotoxic cells, a name coined by us as there was no clear classification. We
63 hypothesized that a subset of T cells might functionally resemble CD4-positive T cells, expressing
64 markers that may indicate their interaction with B cells. However, we did not have sufficient cell
65 numbers for further sub-clustering of the 1,300 T cells.

66 In the current work, we have assembled a much larger dataset of single-cell RNA sequencing
67 (scRNAseq) data of 57 thousand spleen cells from 34 Atlantic cod specimens in a vaccination study.
68 The teleost spleen functions as the primordial secondary lymphoid organ where adaptive immune
69 responses are generated [2]. By sampling from both naive and vaccinated fish before, during, and after
70 an immune challenge, we capture cells in a broad spectrum of immune states. Sub-clustering and
71 pseudotime trajectory analysis of the B cells revealed expression of transcription factors that may be
72 involved in B cell differentiation. Closer inspection of the almost 14 thousand T lymphocytes revealed
73 a large subset that does not express CD8. The majority of CD8-negative T cells express high to
74 extremely high levels of a homolog of *monocyte chemotactic protein 1b* (*mcp1b*), whereas a smaller
75 subset of CD8-negative T cells express a homolog of the scavenger receptor *m130*. The presence of T
76 cell subsets in the Atlantic cod secondary lymphoid organ that express neither *cd4* nor *cd8* co-
77 receptors poses important questions about the functional organisation of the immune system in this
78 species.

81 **2 Methods and materials**

83 **2.1 Atlantic cod sampling**

84 Atlantic cod sampled for this study originate from a single breeding family (bred from 1 female
85 and 2 males) from the NOFIMA breeding program in Tromsø, Norway. They were reared, vaccinated,
86 and challenged at the NIVA Research Facility at Solbergstrand, outside Oslo, Norway. The rearing and
87 sampling were performed according to the European animal welfare regulations and approved by the
88 Norwegian authorities (FOTS ID 21758).

89 Sampling took place between 9 and 11 months of age (average length = 21cm, range 13-
90 27cm). The water temperature was maintained at ~8°C in keeping with the seasonal water
91 temperature, with a water salinity of 34 PSU, light conditions were 12:12 hour light:dark, and the cod
92 were fed with Skretting cod pellets. Spleen samples were taken from 34 Atlantic cod that were used
93 in a vaccination study for *Vibrio anguillarum* (strain O2a ATCC 19264). Samples were taken before and
94 after vaccination priming and boosting, before immune challenge, then day one, seven and 15 after
95 immune challenge for naive and vaccinated fish. Vaccination priming and boost, and immune
96 challenge were carried out by bath immersion. A schematic demonstrating sampling is shown in
97 *Supplementary Figure 1*. Fish were killed by cranial concussion and tissue sampling was conducted
98 within minutes of fish death. As blood was also taken for additional investigations not mentioned in
99 this paper, gill slit could not be carried out. The spleens were removed and placed in PBS-BSA 0.01%
100 solution and kept on ice. Spleen cell suspensions were obtained by gently forcing the tissue through a
101 cell strainer (Falcon, 100 µm) and diluted to 200 cells/ul in fresh PBS-BSA 0.01% solution. All cells were

102 kept in regular microcentrifuge tubes to minimise cell loss and kept on ice for transport and laboratory
103 work.

104

105 **2.2 Single-cell cDNA library preparation and sequencing.**

106 Single-cell RNA sequencing (scRNAseq) and the preparation of the libraries were performed according
107 to published protocols [11-13]. A droplet sequencing generator (Dolomite) individually encapsulated
108 cells with barcoded beads. Libraries were sequenced at the Norwegian Sequencing Centre (Oslo
109 University Hospital), on the NextSeq500 platform with a 75 bp kit, high output mode, with paired end
110 reads. 20 bp were sequenced in Read 1 using a custom sequencing primer
111 (GCCTGTCCGCGAAGCAGTGGTATCAACGCAGAGTAC) and 60 bp in Read 2 with the regular Illumina
112 sequencing primer. The sequencing data is available at the ENA repository with Accession number
113 PRJEB47815.

114 We used the Drop-seq Core Computational Protocol [14] to demultiplex the raw sequencing
115 reads and then map them to the most recent version of the Atlantic cod genome, gadMor3 (RefSeq
116 accession GCF_902167405.1) using STAR alignment. A gene of interest, *gata3*, was present in gadMor2
117 [15] but missing in gadMor3, so the *gata3* gene sequence was manually added to the gadMor3
118 assembly fasta file. The reads were summarised into gene expression matrices using the Drop-seq
119 program 'DigitalExpression'.

120

121

122 **2.3 Pre-processing workflow**

123 The resulting count matrices for each sample were loaded into Seurat (version 4.0.2)[16-19].
124 The count matrices from each of the 34 cod were integrated into one Seurat object through anchor
125 identification using the 'FindIntergationAnchors' and 'IntergrateData' Seurat functions. The
126 percentage of mitochondrial gene expression was added by 'PercentageFeatureSet' and cell barcodes
127 with more than 5% of mitochondrial genes, 'percent.mt' were removed. Cell barcodes with fewer than
128 150 genes and greater than 1500 genes, 'nFeature_RNA', and those that contained genes expressed
129 in less than three cells, 'min.cells', were filtered out. Additionally, cells with a total number of
130 biological molecules greater than 4000, 'nCount_RNA', were removed. These steps reduce the number
131 of low-quality cells and reduce cell multipliers or cell barcodes which do not contain a true cell
132 transcriptome but rather ambient RNA. Following quality control filtering, we derived a gene
133 expression matrix of 19,279 genes across 56,994 splenic cells. An overview of the samples in each
134 treatment group in the immune challenge protocol, sequencing library, average mapping percentages,
135 number of cells, mapped transcripts, and genes are shown in Supplementary excel sheet 1.

136 After filtering, data were normalized using the 'NormalizeData' function, variable features
137 were identified using the 'FindVariableFeatures' function, and features were scaled using the
138 'ScaleData' function. PCA analysis was performed, and the most significant principal components were
139 identified by plotting the first 50 dimensions on an Elbow plot (*Supplementary Figure 2*).

140

141 **2.4 Dimension reduction and assigning cluster identity**

142 Unsupervised dimension reduction was performed using Uniform Manifold Approximation
143 and Projection (UMAP) [20] on the first 40 principal components and the clusters were identified using
144 the 'FindNeighbors' (dims = 1:40) and 'FindClusters' functions (res = 0.2). Cluster identities were
145 assigned by assessing differential expression of marker genes between different clusters using the
146 biomarkers detected from the 'FindAllMarkers' function (only.pos = TRUE, min.pct = 0.25,
147 logfc.threshold = 0.25). The top 20 differentially expressed genes for all clusters found in the splenic
148 samples can be seen in *Supplementary excel sheet 2*.

149 To examine the lymphocyte populations more closely, we selected the B cells, CD8-positive T
150 cells, MCP1b-positive T cells, proliferating lymphocytes, and plasma cells from the global splenic
151 UMAP, thus selecting 23,227 lymphocytic cells. These lymphocytes were then clustered on the first 40
152 dimensions at 0.2 resolution. As a result of this unsupervised clustering step the proliferating

153 lymphocytes cluster was divided into B lymphocytes or T lymphocytes. The 9,474 cells in total
154 identified as B lymphocytes were clustered using UMAP on the first 40 dimensions with a 0.3
155 resolution. The 13,753 cells identified as T lymphocytes were clustered using UMAP on the first 40
156 dimensions with a 0.09 resolution.

157

158 **2.5 Trajectory analysis**

159 We used Slingshot (v. 1.8.0) analysis [21] to infer possible differentiating trajectories within
160 the B lymphocyte sub-clusters. UMAP was used to determine the dimensionality and the lineages were
161 constructed in an unsupervised way. To infer differential gene expression in the lineages predicted by
162 the Slingshot analysis, we used the GAM package (v. 1.20) to run a generalized additive model (GAM)
163 which uses a LOESS term for pseudotime. This identified the top 100 most variable genes across
164 pseudotime (*Supplementary excel sheets 3*). The lineages and expression of key genes were visualised
165 using the Slingshot tools, the ggplot2 (v. 3.3.3) [22] package, and the scater package (v. 1.18.6)[23].
166

166

167 **2.6 Phylogeny analysis of *m130*, *mcp1b*, and *tcr* genes**

168 All gene names reported in the scRNA analyses are derived from the automated annotation of the
169 gadMor3 assembly. To further explore the identity of particular genes of interest, *mcp1b*
170 (LOC115529242), *m130* (LOC115541469) and the *tcr* genes, in more detail, maximum likelihood
171 phylogenetic trees were constructed.

172 Scavenger Receptor Cysteine-Rich Type 1 Protein M130 (CD163) references were collected
173 from the groups Mammalia, Aves, Reptilia, Amphibia and Teleostei at Uniprot.org where available.
174 The predicted gene models of the scRNA-reported annotations were then subjected to a blastp at
175 NCBI towards mammalian and teleostei databases using default parameters. Here, 3-5 hits annotated
176 as M130/M160/CD163 were selected to be included in the multiple sequence alignment. The
177 scavenger receptor cysteine rich (SRCR) domain present in CD163 is an ancient and conserved domain
178 shared by members of the group B SRCR superfamily (Herzig et al., 2010). To provide more framework
179 to the alignment of *m130*, additional members of the group B SRCR family were included (CD5, CD5L
180 and CD6) together with two other scavenger receptors: scavenger receptor cysteine rich family
181 member with 4 domains (SSC4D) and Scavenger Receptor Class B Member 1 (SCARB1), all obtained in
182 the same manner as described above.

183 Monocyte chemotactic protein 1 (CCL2) references were obtained as described above for
184 CD163. Furthermore, as CCL2 is a chemokine belonging to a large gene family, a set of references for
185 the most common CC chemokines in humans and fish were downloaded from genbank and added to
186 the alignment. In addition, some CXC chemokines were added to function as a collective outgroup.
187 Finally, complete CC chemokine characterizations from Channel catfish and Atlantic cod were added,
188 together with all predicted gene models from gadMor3 reported from a tblastn search using the CCL2
189 references, default parameters and e-value cutoff at 1e-1 [24].

190 The final multiple sequence alignments (protein) were aligned using MUSCLE in MEGA7 and
191 default parameters [25]. The resulting protein alignment was subjected to a maximum likelihood run
192 using raxml-ng [26] after model testing using modeltest-ng [27]. For CD163, the best scoring model
193 was WAG+G4 and for CCL2 VT+I+G4. Both maximum likelihood runs were run until convergence and
194 followed with 500 bootstrap replicates.

195 We also constructed a phylogenetic tree of *tcr* genes in Atlantic cod and in other selected
196 species. The annotated *tcrb* (LOC115544273) and *tcrα* (LOC115548821) genes in gadMor3, as well as
197 putative *tcr* genes (LOC115548656 and LOC115548822) identified by blasting gadMor3 with *tcr* genes
198 from different teleosts, reptiles, and birds, were compared. All genes with hits above 1e-100 were
199 collected and added to the overall sequence alignment. A multiple sequence alignment was generated
200 using MEGA7 and its MUSCLE alignment program with default setting. From here a neighbour joining
201 tree using Poisson distribution, pairwise deletion and 200 bootstrap replicates was made again using
202 MEGA7.

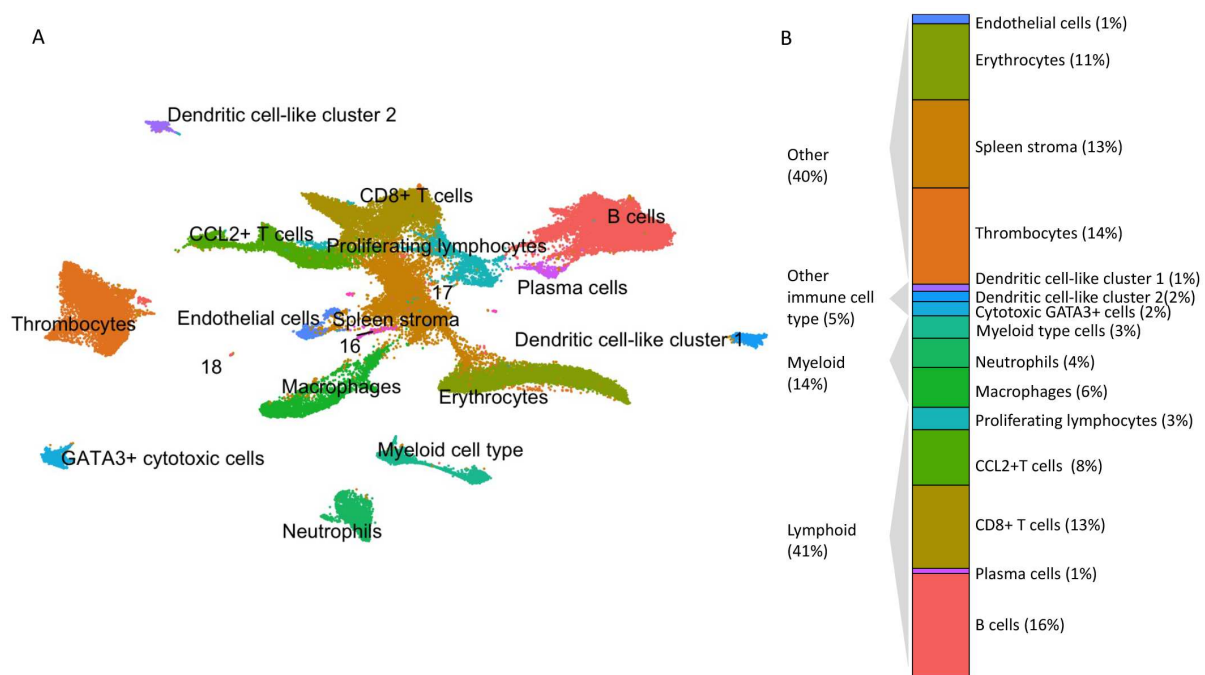
203 The trees are visualized and edited for presentation purposes using FigTree v 1.4.4 [28]

204
205
206
207
208
209
210
211
212
213
214
215
216
217
218

3 Results

3.1 Overview of cells found in Atlantic cod spleen

We analysed spleens from 34 Atlantic cod at 12 timepoints during a vaccination and immune challenge study of *V. anguillarum*, thus capturing a broad immune status. We examined these spleen samples using scRNAseq. In this study we focus on a detailed exploration of cell sub-clusters within the B and T cell lymphocytes, and thus we do not delve into the differing immune responses following vaccination and immune challenge. All the named clusters in the global UMAP in *Figure 1* as well as the larger lymphocyte sub-clusters have cells from all the sampled fish. While some of the smallest lymphocyte sub-clusters are not represented by all fish, there was no pattern of changing sub-cluster population size with respect to naive versus vaccinated fish or along the immune challenge timeline. This demonstrates that all the splenic cell populations and lymphocyte sub-cluster populations are found in both steady state and immune perturbed Atlantic cod. The numbers of cells found in each cluster or sub-cluster is shown in *Supplementary excel sheet 4*.



219
220
221
222
223
224
225
226
227
228
229
230
231
232
233
234
235

Figure 1. Unsupervised clustering of 56,994 Atlantic cod splenic cells reveals a population of CD8-negative T cells.

(A) Single-cell RNA sequencing of splenic cells is visualised in two dimensions using UMAP. Cluster identity was assigned based upon differentially expressed genes and naming from our last publication [11]. Clusters 16-18 each represent less than 0.2% of the total cells and so have not been named.

(B) Bar chart showing percentage of splenic cells as lymphoid cells, myeloid cells, other immune cells, and other splenic cells. Cells from clusters 16-18 have not been included in the percentage calculations.

Following quality control filtering, we derived a gene expression matrix across 56,994 Atlantic cod splenic cells. Visualization of cell types in two dimensions using UMAP revealed 15 cell clusters with distinct gene expression signatures (*Figure 1A*, a list of differentially expressed genes can be viewed in *Supplementary excel sheet 2*). Three clusters, clusters 16, 17, and 18, each represented less than 0.2% of the total cells and so remain unnamed. The splenic cells contained the major types of lymphoid and myeloid cells, minor immune cell types (myeloid cell type, dendritic cell cluster 1 and 2, and GATA3⁺ cytotoxic cells), as well as other cell types (the thrombocytes, erythrocytes, spleen stromal cells, and endothelial cells). The cell cluster 'myeloid cell type' was previously named 'natural killer

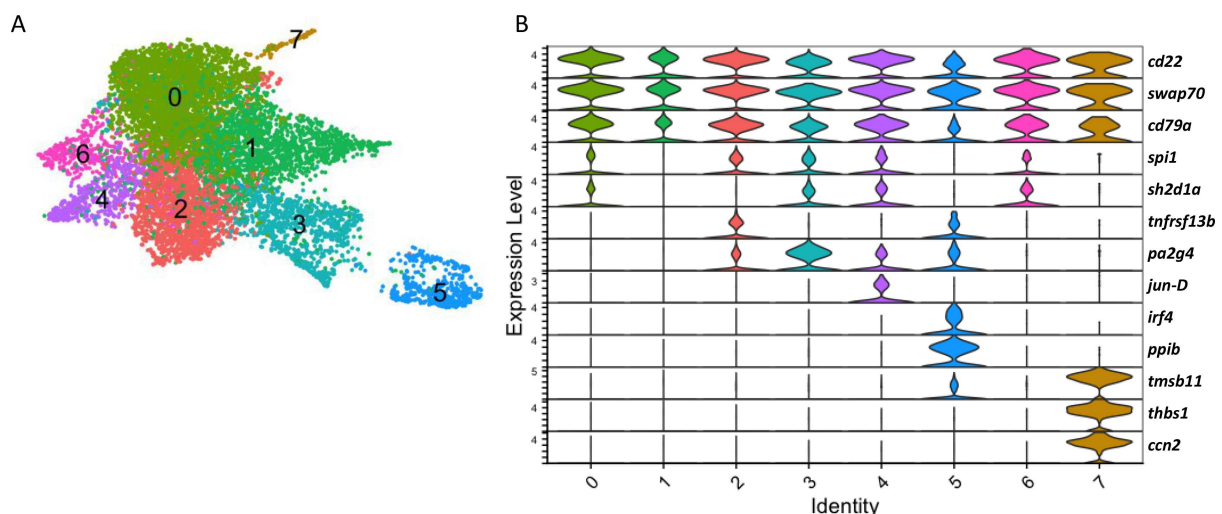
236 cells' by us [11]. Despite a larger sample size in the present study, a lack of clear marker genes has
 237 resulted in a less specific name choice. Two clusters demonstrated gene expression profiles matching
 238 dendritic cells, both expressing the receptor tyrosine kinase *flt3*, allograft inflammatory factor 1 (*aif1*),
 239 and various cathepsin genes, and have thus been named dendritic cell cluster 1 and 2. The naming of
 240 the cell types is otherwise consistent with our first classification of cod immune cells [11].

241 The lymphocytes represented 41% of the splenic cells present, and were made up of B cells,
 242 plasma cells, proliferating lymphocytes, and T cells (*Figure 1B*). The T cells were clustered into two
 243 distinct groups; one group contains CD8-positive T cells, while the other did not show CD8 expression
 244 but highly expressed a homolog of *mcp1b*, thus given the name MCP1b-positive T cells (*Figure 1A*).
 245 The myeloid cells (containing the macrophages, neutrophils, and myeloid type cells) represented 14%
 246 of splenic cells, while the other immune cells (Dendritic cell cluster 1, Dendritic cell cluster 2, and
 247 GATA3⁺ cytotoxic cells) represented 5% of splenic cells (*Figure 1B*).
 248

249 3.2 B lymphocyte sub-clusters

250 By selecting 9,474 B lymphocytic cells (the B cells, B cells within the proliferating lymphocytes,
 251 and plasma cells) from the global UMAP containing all splenic cells and re-clustering these cells at a
 252 higher resolution, eight sub-clusters were revealed (*Figure 2A*). Shared expression of the marker genes
 253 *cd22*, *swap70*, *cd79a* (*Figure 2B*) and immunoglobulin genes (*Supplementary Figure 3*) confirmed
 254 these were all B lymphocytes. B cell sub-clusters 0, 1, 2, 3, 4, and 6 were not conspicuously different
 255 from one another, revealing a mixed gradient pattern of gene expression, such as the transcription
 256 factors *spi1* and the adapter protein *sh2d1a* (*Figure 2B*). Sub-clusters 2 and 5 expressed the TNF
 257 receptor super-family gene *tnfrsf13b*. The expression of shared immunoglobulin genes dominated the
 258 most significantly expressed genes for these clusters, with few unique marker genes (*Supplementary*
 259 *excel sheet 5*). B cell sub-cluster 4 differentially expressed *jun-D*, a sub-unit of the AP-1 transcription
 260 factor, which has been linked to different roles in B cell activation and differentiation [29].

261 B cell sub-clusters 5 and 7 had very distinct gene expression profiles. Sub-cluster 5, making up
 262 5% of the B cells, are the previously identified plasma cells and expressed the marker genes *interferon*
 263 *regulatory factor 4* (*irf4*) and *peptidylprolyl isomerase b* (*ppib*) (*Figure 2B*) and demonstrated the
 264 highest average expression of immunoglobulin genes (*Supplementary Figure 3*), as expected. B cell
 265 sub-cluster 7, making up only 1% of the B cells, highly differentially expressed several genes, including
 266 *thrombospondin 1* (*thbs1*), *thymosin beta 11* (*tmsb11*), and *cellular communication network factor 2*
 267 (*ccn2*) (other genes can be seen in *Supplementary excel sheet 5*).



268 Figure 2. Closer examination of 9,474 Atlantic cod B lymphocytes reveals 8 sub-clusters with distinct
 269 transcriptome profiles.

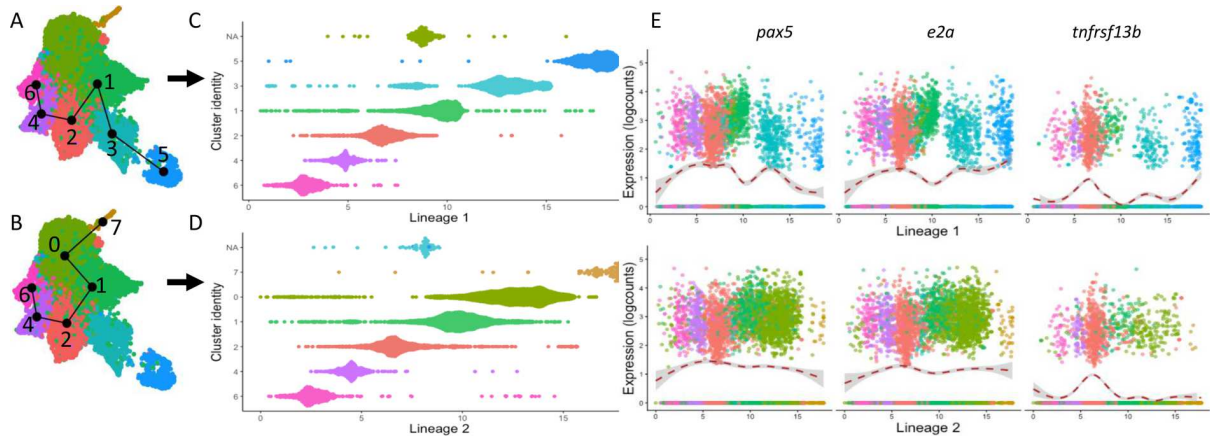
270 (A) Visualization of B lymphocyte cells using UMAP.

271 **(B)** Violin plots showing expression of selected genes identified by differentially expressed gene
 272 analysis. The y-axis indicates normalized and log-transformed average expression of the selected
 273 genes and the x-axis indicates the B cell sub-cluster.

274

275 The trajectory analysis Slingshot is an inference tool which computationally orders cell clusters
 276 along a predicted developmental trajectory based on gene expression, an ordering known as
 277 pseudotime. Performing a Slingshot analysis on the B lymphocyte clusters suggested two lineages;
 278 both lineages started in B cell sub-cluster 6, with lineage 1 ending in sub-cluster 5 (the plasma cells)
 279 and lineage 2 ending in sub-cluster 7 (*Figure 3A-D*). We did not manually select any start or end points
 280 for the lineages, allowing Slingshot to compute pseudotime in an unbiased fashion. The terminal
 281 clusters of the two lineages are consistent with the discrete populations demonstrated by the
 282 differential gene analysis. B cell sub-cluster 3, which is the cluster of B cells ordered in pseudotime
 283 right before the terminally differentiated plasma cells, highly expressed *proliferation associated 2g4*
 284 (*pa2g4*), a gene involved in cell proliferation, differentiation, and survival [30].

285 We fit a generalised additive model (GAM) to the two predicted trajectories to explore
 286 potential differences in the progression of the B cell lineages and identified the top 100 temporally
 287 expressed genes (*Supplementary excel sheet 3*). The expression of these genes changed in a
 288 continuous manner over pseudotime. The transcription factors *pax5* and *e2a* were present among the
 289 top differentially expressed genes identified by GAM and visualised as smooth expression plots (*Figure*
 290 *3E*). The gene *tnfrsf13b* is a gene of biological interest and has also been shown. All three genes are
 291 linked to B cell development: *pax5* encodes the B cell lineage-specific activator protein expressed at
 292 early stages of B cell differentiation [31], *e2a* plays a role in B and T lymphocyte development [32],
 293 and *tnfrsf13b* encodes the transmembrane activator and CAML interactor (TACI) suggested to control
 294 B cell differentiation and memory [33, 34]. At the end of lineage 1 the expression levels of *pax5*
 295 dropped in the plasma cells, while expression levels of *e2a* and *tnfrsf13b* both showed an increase. In
 296 lineage 2 the expression levels of the *pax5* and *e2a* remained steady, while expression of *tnfrsf13b*
 297 peaked in sub-cluster 2 and then had low expression through the rest of the lineage. It is unclear why
 298 there was a noticeable dip in expression level of all *pax5* and *e2a* genes in sub-cluster 1, especially in
 299 lineage 1.



300 Figure 3. Pseudotime analysis of B lymphocyte cells reveal two lineages with different expression
 301 patterns of transcription factors.

302 **(A + B)** B cell sub-clusters depicting the Slingshot-predicted lineage trajectories, lineage 1 **(A)**
 303 terminating in the B cell sub-cluster 5 (the plasma cells), and lineage 2 **(B)** terminating in B cell
 304 sub-cluster 7.

305 **(C + D)** Depiction of cells within each B cell sub-cluster from the Slingshot-predicted lineage on the y-
 306 axis along pseudo-temporal ordering on the x-axis. Each dot represents a cell and its predicted
 307 temporal position in development in lineage 1 **(C)** and lineage 2 **(D)**.

308 **(E)** Smoothed expression plots along B lymphocyte lineages for the transcription factors *pax5*, *e2a*,
 309 and *tnfrsf13b*. Each point represents the expression level of each transcript within a single cell. The

310 colour is consistent with the sub-cluster identity. The red dashed line is a weighted regression to fit a
311 smooth curve through the points (LOESS curve), and the grey area shows a 95% confidence interval.

312

313 **3.3 Phylogenetic overview of *m130*, *mcp1b* and *tcr* genes**

314 The phylogenetic tree of *m130* (*Supplementary Figure 4A*) cannot with confidence confirm
315 that the suggested *m130* gene model from the annotation is indeed CD163 as the support within the
316 backbone of the phylogeny was too low. However, there was support to place the gene model within
317 the *group B scavenger receptor cysteine-rich (SRCR) superfamily* and that the gene model was closer
318 to CD163/CD163L than the other superfamily members, making it a CD163-like candidate. Thus, we
319 would describe the gene model *m130* as a scavenger receptor superfamily member that may have
320 CD163-like functions. The classical CD163 property is the ability to bind and internalise low density
321 lipoproteins [35], such as the haemoglobin-haptoglobin complex [36].

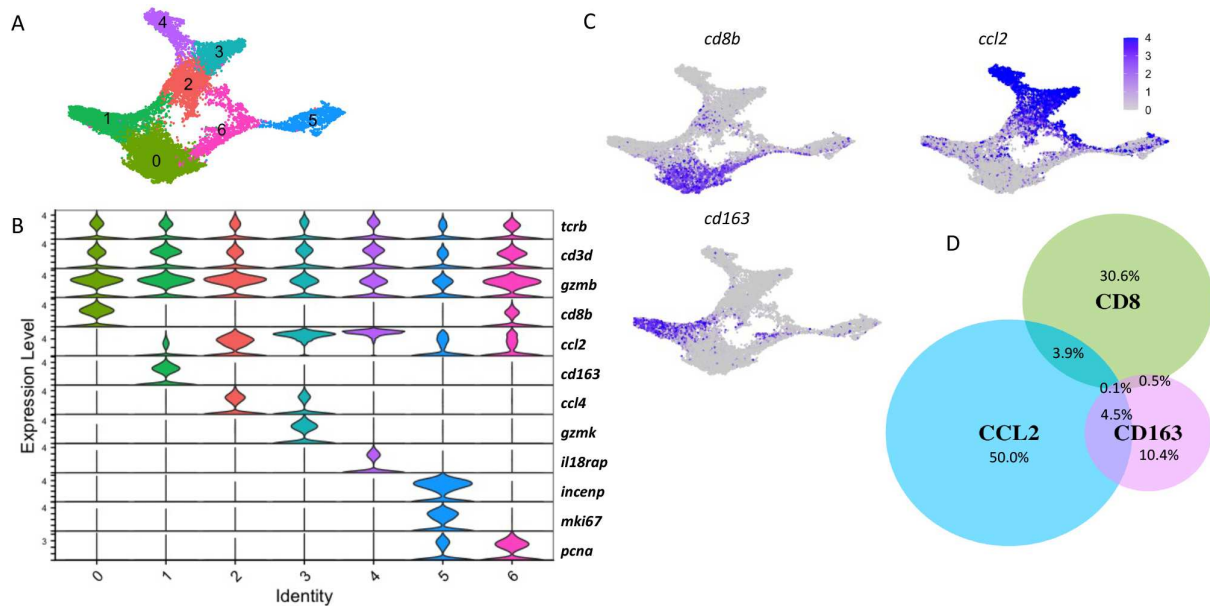
322 The proposed *mcp1b* gene model clustered together with several other characterized CC
323 chemokines from Atlantic cod (*Supplementary Figure 4B*). However, the tree did not resolve beyond
324 clustering the major chemokine family members together, the CC and CXC chemokines respectively,
325 and overall displayed no bootstrap support in the backbone of the phylogeny. This indicated that
326 the *mcp1b/CCL2* annotation of the gene model is inaccurate and further characterization of the gene
327 model is needed. We would thus describe this gene model as a CC chemokine of unknown function.

328 Phylogenetic analysis of the annotated *tcr* genes *tcra* (LOC115548821) and *tcrb*
329 (LOC115544273) supported the identity of these genes, while LOC115548656 was grouped with
330 known *tcrg* genes and LOC115548822 was grouped with known *tcrd* genes, suggesting that these two
331 genes represent Atlantic cod *tcrg* and *tcrd*, respectively (*Supplementary Figure 4C*)

332

333 **3.4 T lymphocyte sub-clusters**

334 Selecting the 13,753 T lymphocyte cells from the global UMAP and re-clustering them
335 revealed five T cell sub-clusters with distinct gene expression profiles in each (*Figure 4A, 4B and 4C*).
336 Expression of *tcr* genes, *cd3d*, and the *cytotoxic granzyme B (gzmb, LOC115532977)* genes within the
337 13,753 cells confirmed all these clusters are T lymphocytes (*Figure 4B*). All T cell clusters, except sub-
338 cluster 2, expressed similar levels of *tcra* and *tcrb*. Sub-cluster 2 cells expressed *tcrb* but did not express
339 *tcra*, but instead expressed putative *tcrg* and putative *tcrd*. This cluster also expressed a homolog of
340 *m130* (*Supplementary Figure 4B*), a scavenger receptor also known as CD163 that is typically
341 considered a marker of activated or anti-inflammatory macrophages [37]. T cell sub-cluster 0 was CD8-
342 positive and expressed CC chemokine receptor 7 (*ccr7*) and a second granzyme B paralogue (*gzmb*,
343 LOC115532976). Sub-clusters 1 and 4 expressed *mcp1b* in especially high levels in comparison to the
344 other sub-clusters. Sub-cluster 1 expressed the chemokine *ck5b (ccl4)* and granzyme k, *gzmk*, while
345 cluster 4 expressed interleukin 18 receptor accessory protein, *il18rap*. T cell sub-cluster 3 expressed
346 the proliferation markers *mki67* and *pcna*, as well as *incenp*, a regulator of mitosis. The top
347 differentially expressed genes of each T cell sub-cluster can be seen in *Supplementary excel sheet 6*.
348 In summary, although five T cell sub-clusters were revealed by the UMAP, it was noticeable that there
349 were three distinct T cell populations: a population which expressed *cd8* (sub-cluster 0), a population
350 which expressed *mcp1b* (sub-clusters 1 and 4), and a population which expressed *m130* (sub-cluster
351 2) (*Figure 4B, 4C and 4D*). Sub-cluster 3 represented proliferating T cells, but their relationship to the
352 other three T cell populations remains inconclusive.



354 Figure 4. Closer examination of 13,753 Atlantic cod T lymphocyte cells reveals 5 sub-clusters with
 355 distinct transcriptome profiles. Expression of T cell co-receptor *cd8b*, cytokine *mcp1b*, and the
 356 scavenger receptor *m130* segregates T lymphocytes into three distinct sub-populations.

357 **(A)** Visualization of T lymphocyte cells using UMAP reveals five T cell sub-clusters.

358 **(B)** Violin plots showing expression of selected genes identified by differential expressed gene analysis.
 359 The *y-axis* indicates normalized and log-transformed average expression of the selected genes and the
 360 *x-axis* indicates the T cell sub-cluster identity.

361 **(C)** UMAP showing the expression level of *cd8b*, *mcp1b*, and *m130* in T lymphocytes. Cells are coloured
 362 by expression level.

363 **(D)** Venn diagram demonstrating that the expression of *cd8b*, *mcp1b*, and *m130* is largely non-
 364 overlapping. The percentage of T cells expressing each gene is shown.

365

366 Given the knowledge at hand, we re-analysed the T lymphocytes in our first scRNAseq dataset
 367 of cod immune cells [11] and searched for the same genes shown in Figure 4B. We again found that
 368 *cd8*, *m130*, and *mcp1b* were expressed in three mutually exclusive populations (*Supplementary Figure*
 369 *5*), echoing the results shown here. This pattern was also seen in the global UMAP containing all the
 370 splenic cells (*Supplementary Figure 6*).

371 The only other cells in the spleen to express *mcp1b* or *m130* was the GATA3⁺ cytotoxic cells
 372 (*Supplementary Figure 6*). *gata3* is a master regulator of T helper 2 cells in mammals [38, 39] and has
 373 also been shown to play a role in the development of innate lymphoid cells [40]. This cluster was
 374 identified and named in our previous paper [11], and, consistent with our previous description, did
 375 not express other T cell markers, supporting our previous hypothesis that this cluster represents an
 376 innate lymphoid cell type.

377

378 **4 Discussion**

379

380 Multiple genome studies, as exemplified by several teleosts, have revealed a plasticity and
 381 adaptability of the vertebrate adaptive immune system. The Atlantic cod [3], and later the entire
 382 Gadiformes lineage [4], was shown to have lost the MHC-II/CD4 T cell pathway. Further peculiarities
 383 have been found in other teleost species, including the loss of MHC-II/CD4 in pipefish [41, 42] and
 384 monkfish [43], and the loss of MHC-II/CD4 alone or in combination with the loss of MHC-I/CD8 in
 385 several deep-sea species of anglerfish [44]. In the absence of specific antibodies, it is difficult to assess
 386 the immune cell composition as a first step towards understanding the immune system adaptations
 387 that have occurred in these newly identified adaptive immune systems. Transcriptomic analysis at the

388 single cell level is a powerful tool that we have used successfully in characterising immune cell
389 populations of the Atlantic cod [11]. In this study, we have vastly increased the number of immune
390 cells studied by scRNAseq, to 57 thousand spleen cells from 34 fish that were sampled during a
391 vaccination and immune challenge study, compared with a total of 7 thousand blood and spleen cells
392 from two fish in our previous study. The increased number of cells gave us the power to scrutinise in
393 detail the B cell and T cell subsets found within 9,474 B cells and 13,753 T cells that were included in
394 the current study.

395 Unsupervised sub-clustering of B lymphocytes revealed eight B cell sub-clusters, of which the
396 sub-clusters 5 and 7 are transcriptionally most distinct. Sub-cluster 5 is identical with the plasma cell
397 subset that was identified in the global analysis, which included all splenocytes. Trajectory analysis by
398 Slingshot suggested a common maturation / differentiation pathway of B cells encompassing the first
399 four common progenitor B cell sub-clusters, and then diverging into two separate trajectories each
400 ending up in the presumed end-differentiated B cell sub-cluster 5 (the plasma cells) and sub-cluster 7.
401 That one trajectory ends in the plasma cells, a well-established terminally differentiated cell type,
402 gives strength to the unsupervised ordering of the clusters by Slingshot. In addition, B cell sub-cluster
403 3, the penultimate sub-cluster in the plasma cell lineage, highly expresses *pa2g4*, a gene involved in
404 cell proliferation and differentiation, further strengthening the trajectory analysis. B cell sub-cluster
405 7, which is the end point of the other trajectory makes up only 1% of the B lymphocytes. This cluster
406 expresses *thbs1*, *tmsb11* and *ccn2* at a high level, which leads us to speculate that this small subset of
407 highly differentiated B cells may have effector functions that involve communication with other cells.
408 This functionally differentiates this cluster from plasma cells, whose function involves antibody
409 production, and so may be more in line with the regulatory functions of certain B cell subsets that
410 have been recently suggested in mammalian immunology [45]. Functional confirmation of this sub-
411 cluster of B cells is needed when appropriate reagents become available.

412 The most remarkable finding in the T lymphocyte population is the absence of T cell co-
413 receptor *cd8* expression in several subset, accounting for 65% of all T cells. The majority of the CD8-
414 negative T cells are positive for a CC chemokine initially annotated as *MCP1b*. However, great
415 differences exist between fish and mammalian cytokines, and within fish species, making annotation
416 of cytokines extremely problematic [46-48]. The sequence phylogeny of *mcp1b* gives support that this
417 gene is a C-C motif chemokine but gives little to support this gene model is MCP-1/CCL2. Cytokines
418 rapidly adapt in species and also experience prevalent gene losses and expansions [48]. Lacking
419 functional data and a clear naming alternative we have kept the naming given in *gadMor3*: *mcp1b*.
420 MCP-1 is a chemoattractant for monocytes and T cells in humans [49]. In humans and mice, the main
421 producers of MCP-1 are myeloid cells (monocytes and macrophages) [50], in addition it is also
422 produced by some non-immune cells such as epithelial and endothelial cells [51]. In our scRNAseq
423 data of the Atlantic cod spleen, we find that *mcp1b* is primarily expressed by T cells and GATA3⁺
424 cytotoxic cells, and we do not find *mcp1b* expression in the myeloid or stromal cells present in the
425 spleen, further suggesting that *mcp1b* as expressed in Atlantic cod is different from the role of MCP-1
426 in mammals and does not fulfil the same role. We do not know which genes encode the receptor(s)
427 for *mcp1b* in cod, or which cells that express them. It is intriguing to note that although the expression
428 of *gzmb* is uniformly high in all T-cell sub-clusters, the *gzmb* expression is nevertheless lower in the
429 two sub-clusters, 3 and 4, that show extremely high levels of *mcp1b*. It is thus tempting to speculate
430 that cells in these two sub-clusters have reduced cytotoxic functions and rather may be devoted to
431 signalling with other not-yet identified immune cells through its secretion of the chemokine *mcp1b*.

432 Most of the T cells which are negative for both CD8 and MCP1b express *m130*. Phylogenetic
433 comparisons of this gene demonstrated that *m130* clustered within the group B SRCR superfamily,
434 and we propose it is CD163-like. In humans and rodents, CD163 is found to be expressed exclusively
435 in cells of monocytic origin [52], which is not found here. The B SRCR superfamily is an ancient and
436 conserved protein domain, and some orthologues genes within this family, CD163c- α -like/WC1, have
437 been shown to play a role in the regulation of gamma delta T cells in cattle [53].

438 In our scRNAseq data from cod spleen, *cd8*, *mcp1b*, and *m130* are expressed in T lymphocytes
439 in a largely exclusive manner, giving rise to three distinct and separate T cell sub-populations. The
440 CD8-positive, MCP1b-positive, and M130-positive populations all express key T cell markers, such as
441 *cd3*, *tcg* genes, and *gzmb* (Figure 4A). There are two developmental scenarios for these three distinct
442 populations: they have either acquired the expression of their respective markers during
443 lymphogenesis in the thymus and exit thymus as three populations of mature T cells that do not
444 interconvert in the periphery; or that they all evolve from the same mature progenitor T cells and
445 represent three differentiation stages. The finding that M130-positive cells uniquely express two
446 genes putatively suggested to be *tcrg* and *tcrd*, indicates that the M130-positive cells represent a
447 separate lineage of T cells. More detailed molecular analysis such as full-length TCR sequencing is
448 needed to ascertain whether these cells may represent gamma delta T cells, the existence of which
449 has not been demonstrated in cod before. Likewise, scRNAseq combined with single-cell TCR
450 sequencing may also reveal the developmental relationship between the various T cell sub-
451 populations, as well as whether some sub-clusters may contain unconventional T cells similar to
452 natural killer T cells or mucosal associated invariant T cells that show restricted and semi-invariant V-
453 gene usage in mammalian systems [54, 55]. The CD8-positive population uniquely expresses
454 chemokine receptor *ccr7* suggesting this subset may have a different trafficking pattern than the other
455 CD8-negative T cell subsets.

456 The B and T cell differentiation pathways in teleosts are poorly understood, and there may be
457 substantial differences between different lineages of teleosts. An alternative to use of classical surface
458 markers is to identify transcription factors which are differentially expressed along predicted lineages.
459 *pax5* and *e2a* are well-known genes participating in B cell differentiation and activation [31, 32], and
460 have even been identified in teleost B cell lymphogenesis [56]. *pax5* and *e2a* are among the top
461 differentially expressed genes in the predicted B cell lineages in this study, suggesting these genes also
462 play an important role in B cell differentiation in the Atlantic cod. Expression of the gene *tnfrsf13b* was
463 shown to be increased in the cod plasma cells, results in alignment with human studies suggesting
464 *tnfrsf13b* has a role in the development of plasma cells and production of much of the Ig in blood [33,
465 34]. The TACI surface receptor encoded by this gene is suggested to be involved in T cell-independent
466 antibody responses [57], which is interesting given the absence of CD4 T helper cells in cod.

467 It is interesting to note that the two novel T cell population markers we have discussed here,
468 namely *m130* and *mcp1b*, are only expressed in the GATA3⁺ cytotoxic cell population in addition to
469 the T cells. Despite sharing these unique markers, the GATA3⁺ cytotoxic cells do not express *tcg* and
470 are transcriptionally distant from the other lymphocyte clusters, as visualised by the global UMAP, and
471 so we cannot classify them as T cells. We previously hypothesised these cells represent a population
472 of innate lymphoid cells [11], and the additional findings here make this a population of interest for
473 future studies.

474 Here we present a refined characterisation of the T and B lymphocytes in the Atlantic cod
475 spleen using single-cell transcriptomics. The discovery of novel T cell subset markers gives guidance
476 to the future direction of studying T cell development, differentiation, and function in Atlantic cod. In
477 addition, the trajectories analysis reveals candidate transcription factors that drive B cell
478 differentiation. These hypotheses need to be validated in future studies.

479
480

481 **5 Acknowledgements**

482 Financing from the “comparative immunology of fish and humans (COMPARE)” project at the
483 University of Oslo.

484 In collaboration with the “rational design of vaccination strategies for Atlantic cod (VACSACOD)”
485 program, Research council of Norway.

486 Norwegian Sequencing Centre provided sequencing services.

487 We thank Henning Sørum (Norwegian University of Life Sciences) for discussion and planning of the
488 immunisation experiments.

489
490
491
492
493
494
495
496
497
498
499
500
501
502
503
504
505
506
507
508
509
510
511
512
513
514
515
516
517
518
519
520
521
522
523
524
525
526
527
528
529
530
531
532
533
534
535
536
537
538

6 References

1. Schluter, S.F., et al., *'Big Bang' emergence of the combinatorial immune system*. Dev Comp Immunol, 1999. **23**(2): p. 107-11.
2. Flajnik, M.F., *A cold-blooded view of adaptive immunity*. Nat Rev Immunol, 2018. **18**(7): p. 438-453.
3. Star, B., et al., *The genome sequence of Atlantic cod reveals a unique immune system*. Nature, 2011. **477**: p. 207.
4. Malmstrom, M., et al., *Evolution of the immune system influences speciation rates in teleost fishes*. Nat Genet, 2016. **48**(10): p. 1204-1210.
5. Pilström, L., G.W. Warr, and S. Strömberg, *Why is the antibody response of Atlantic cod so poor? The search for a genetic explanation*. Fish Sci, 2005. **71**(5): p. 961-971.
6. Lund, V., S. Bordal, and M.B. Schroder, *Specificity and durability of antibody responses in Atlantic cod (*Gadus morhua* L.) immunised with *Vibrio anguillarum* O2b*. Fish Shellfish Immun, 2007. **23**(4): p. 906-910.
7. Caipang, C.M.A., M.F. Brinchmann, and V. Kiron, *Profiling gene expression in the spleen of Atlantic cod, *Gadus morhua* upon vaccination with *Vibrio anguillarum* antigen*. Comp Biochem Phys A, 2009. **153**(3): p. 261-267.
8. Gudmundsdottir, S., et al., *Specific and natural antibody response of cod juveniles vaccinated against *Vibrio anguillarum**. Fish Shellfish Immun, 2009. **26**(4): p. 619-624.
9. Magnadottir, B., et al., *Natural antibodies of cod (*Gadus morhua* L.): Specificity, activity and affinity*. Comp Biochem Phys B 2009. **154**(3): p. 309-316.
10. Mikkelsen, H., et al., *Vibriosis vaccines based on various sero-subgroups of *Vibrio anguillarum* O2 induce specific protection in Atlantic cod (*Gadus morhua* L.) juveniles*. Fish Shellfish Immun, 2011. **30**(1): p. 330-339.
11. Guslund, N.C., et al., *Single-Cell Transcriptome Profiling of Immune Cell Repertoire of the Atlantic Cod Which Naturally Lacks the Major Histocompatibility Class II System*. Front Immunol, 2020. **11**: p. 559555.
12. Macosko, E. and M. Goldman. *Drop-seq laboratory protocol*. 2015; Available from: <http://mccarrolllab.org/dropseq/Online-Dropseq-Protocol-v.-3.1-Dec-2015.pdf>.
13. Macosko, Evan Z., et al., *Highly Parallel Genome-wide Expression Profiling of Individual Cells Using Nanoliter Droplets*. Cell, 2015. **161**(5): p. 1202-1214.
14. Namesh, J. *Drop-seq core computational protocol version 1.0.1*. 2015; Available from: <http://mccarrolllab.org/wp-content/uploads/2016/03/Drop-seqAlignmentCookbookv1.2Jan2016.pdf>.
15. Torresen, O.K., et al., *An improved genome assembly uncovers prolific tandem repeats in Atlantic cod*. BMC Genomics, 2017. **18**(1): p. 95.
16. Hao, Y., et al., *Integrated analysis of multimodal single-cell data*. Cell, 2021. **184**(13): p. 3573-3587 e29.
17. Stuart, T., et al., *Comprehensive Integration of Single-Cell Data*. Cell, 2019. **177**(7): p. 1888-1902 e21.
18. Butler, A., et al., *Integrating single-cell transcriptomic data across different conditions, technologies, and species*. Nat Biotechnol, 2018. **36**(5): p. 411-420.
19. Satija, R., et al., *Spatial reconstruction of single-cell gene expression data*. Nat Biotechnol, 2015. **33**(5): p. 495-502.

- 539 20. McInnes, L., et al., *UMAP: Uniform Manifold Approximation and Projection*. Journal
540 of Open Source Software, 2018. **3**: p. 861.
- 541 21. Street, K., et al., *Slingshot: cell lineage and pseudotime inference for single-cell*
542 *transcriptomics*. BMC Genomics, 2018. **19**(1): p. 477.
- 543 22. Villanueva, R.A.M. and Z.J. Chen, *ggplot2: Elegant Graphics for Data Analysis, 2nd*
544 *edition*. Measurement-Interdisciplinary Research and Perspectives, 2019. **17**(3): p. 160-
545 167.
- 546 23. McCarthy, D.J., et al., *Scater: pre-processing, quality control, normalization and*
547 *visualization of single-cell RNA-seq data in R*. Bioinformatics, 2017. **33**(8): p. 1179-
548 1186.
- 549 24. Camacho, C., et al., *BLAST+: architecture and applications*. BMC Bioinformatics,
550 2009. **10**: p. 421.
- 551 25. Kumar, S., G. Stecher, and K. Tamura, *MEGA7: Molecular Evolutionary Genetics*
552 *Analysis Version 7.0 for Bigger Datasets*. Molecular Biology and Evolution, 2016.
553 **33**(7): p. 1870-1874.
- 554 26. Kozlov, A.M., et al., *RAxML-NG: a fast, scalable and user-friendly tool for maximum*
555 *likelihood phylogenetic inference*. Bioinformatics, 2019. **35**(21): p. 4453-4455.
- 556 27. Darriba, D., et al., *ModelTest-NG: A New and Scalable Tool for the Selection of DNA*
557 *and Protein Evolutionary Models*. Molecular Biology and Evolution, 2019. **37**(1): p.
558 291-294.
- 559 28. Rambaut. 2009; Available from: <https://github.com/rambaut/figtree/>.
- 560 29. Shaulian, E. and M. Karin, *AP-1 as a regulator of cell life and death*. Nat Cell Biol,
561 2002. **4**(5): p. E131-6.
- 562 30. Liu, Z., et al., *Ebp1 isoforms distinctively regulate cell survival and differentiation*.
563 Proc Natl Acad Sci U S A, 2006. **103**(29): p. 10917-22.
- 564 31. Cobaleda, C., et al., *Pax5: the guardian of B cell identity and function*. Nat Immunol,
565 2007. **8**(5): p. 463-70.
- 566 32. Kwon, K., et al., *Instructive role of the transcription factor E2A in early B*
567 *lymphopoiesis and germinal center B cell development*. Immunity, 2008. **28**(6): p. 751-
568 62.
- 569 33. Tsuji, S., et al., *TAC1 deficiency impairs sustained Blimp-1 expression in B cells*
570 *decreasing long-lived plasma cells in the bone marrow*. Blood, The Journal of the
571 American Society of Hematology, 2011. **118**(22): p. 5832-5839.
- 572 34. Tsuji, S., et al., *TAC1 deficiency enhances antibody avidity and clearance of an*
573 *intestinal pathogen*. The Journal of clinical investigation, 2014. **124**(11): p. 4857-4866.
- 574 35. Brown, M.S. and J.L. Goldstein, *Receptor-mediated endocytosis: insights from the*
575 *lipoprotein receptor system*. Proceedings of the National Academy of Sciences of the
576 United States of America, 1979. **76**(7): p. 3330-3337.
- 577 36. Kristiansen, M., et al., *Identification of the haemoglobin scavenger receptor*. Nature,
578 2001. **409**(6817): p. 198-201.
- 579 37. Abraham, N.G. and G. Drummond, *CD163-Mediated hemoglobin-heme uptake*
580 *activates macrophage HO-1, providing an antiinflammatory function*. Circ Res, 2006.
581 **99**(9): p. 911-4.
- 582 38. Lee, G.R., P.E. Fields, and R.A. Flavell, *Regulation of IL-4 Gene Expression by Distal*
583 *Regulatory Elements and GATA-3 at the Chromatin Level*. Immunity, 2001. **14**(4): p.
584 447-459.
- 585 39. Yagi, R., J. Zhu, and W.E. Paul, *An updated view on transcription factor GATA3-*
586 *mediated regulation of Th1 and Th2 cell differentiation*. Int immunol, 2011. **23**(7): p.
587 415-420.

- 588 40. Tindemans, I., et al., *GATA-3 Function in Innate and Adaptive Immunity*. *Immunity*,
589 2014. **41**(2): p. 191-206.
- 590 41. Haase, D., et al., *Absence of major histocompatibility complex class II mediated*
591 *immunity in pipefish, Syngnathus typhle: evidence from deep transcriptome*
592 *sequencing*. *Biol Lett*, 2013. **9**(2): p. 20130044.
- 593 42. Roth, O., et al., *Evolution of male pregnancy associated with remodeling of canonical*
594 *vertebrate immunity in seahorses and pipefishes*. *Proc Natl Acad Sci U S A*, 2020.
595 **117**(17): p. 9431-9439.
- 596 43. Dubin, A., et al., *Complete loss of the MHC II pathway in an anglerfish, Lophius*
597 *piscatorius*. *Biol Lett*, 2019. **15**(10): p. 20190594.
- 598 44. Swann, J.B., et al., *The immunogenetics of sexual parasitism*. *Science*, 2020.
599 **369**(6511): p. 1608-1615.
- 600 45. Shang, J., H. Zha, and Y. Sun, *Phenotypes, Functions, and Clinical Relevance of*
601 *Regulatory B Cells in Cancer*. *Front Immunol*, 2020. **11**: p. 582657.
- 602 46. Buchmann, K., *Evolution of Innate Immunity: Clues from Invertebrates via Fish to*
603 *Mammals*. *Front Immunol*, 2014. **5**: p. 459.
- 604 47. Zhu, L.Y., et al., *Advances in research of fish immune-relevant genes: a comparative*
605 *overview of innate and adaptive immunity in teleosts*. *Dev Comp Immunol*, 2013. **39**(1-
606 2): p. 39-62.
- 607 48. Bird, S. and C. Tafalla, *Teleost Chemokines and Their Receptors*. *Biology (Basel)*,
608 2015. **4**(4): p. 756-84.
- 609 49. Carr, M.W., et al., *Monocyte chemoattractant protein 1 acts as a T-lymphocyte*
610 *chemoattractant*. *Proc Natl Acad Sci U S A*, 1994. **91**(9): p. 3652-6.
- 611 50. Yoshimura, T., et al., *Human monocyte chemoattractant protein-1 (MCP-1). Full-*
612 *length cDNA cloning, expression in mitogen-stimulated blood mononuclear leukocytes,*
613 *and sequence similarity to mouse competence gene JE*. *FEBS Lett*, 1989. **244**(2): p.
614 487-93.
- 615 51. Deshmane, S.L., et al., *Monocyte chemoattractant protein-1 (MCP-1): an overview*. *J*
616 *Interferon Cytokine Res*, 2009. **29**(6): p. 313-26.
- 617 52. Barbe, E., et al., *Characterization and expression of the antigen present on resident rat*
618 *macrophages recognized by monoclonal antibody ED2*. *Immunobiology*, 1990. **182**(1):
619 p. 88-99.
- 620 53. Herzig, C.T.A., et al., *Evolution of the CD163 family and its relationship to the bovine*
621 *gamma delta T cell co-receptor WCI*. *BMC Evolutionary Biology*, 2010. **10**(1): p. 181.
- 622 54. Bendelac, A., et al., *MOUSE CD1-SPECIFIC NK1 T CELLS: Development, Specificity,*
623 *and Function*. *Annual Review of Immunology*, 1997. **15**(1): p. 535-562.
- 624 55. Treiner, E., et al., *Selection of evolutionarily conserved mucosal-associated invariant*
625 *T cells by MRI*. *Nature*, 2003. **422**(6928): p. 164-169.
- 626 56. Zwollo, P., *Dissecting teleost B cell differentiation using transcription factors*. *Dev*
627 *Comp Immunol*, 2011. **35**(9): p. 898-905.
- 628 57. von Bülow, G.U., J.M. van Deursen, and R.J. Bram, *Regulation of the T-independent*
629 *humoral response by TACI*. *Immunity*, 2001. **14**(5): p. 573-82.
- 630

Supplementary Files

This is a list of supplementary files associated with this preprint. Click to download.

- [Supplementaryexcelsheets.xlsx](#)
- [Supplementaryfigures.pdf](#)